THE JOURNAL OF PHYSICAL CHEMISTRY B

Article

pubs.acs.org/JPCB

Perturbation of the Redox Site Structure of Cytochrome *c* Variants upon Tyrosine Nitration

H. Khoa Ly,[†] Tillmann Utesch,[†] Irene Díaz-Moreno,[‡] José M. García-Heredia,[‡] Miguel Ángel De La Rosa,[‡] and Peter Hildebrandt*[,†]

[†]Institut für Chemie, Technische Universität Berlin, Sekr. PC14, Straße des 17 Juni 135, D-10623 Berlin, Germany

[‡]Instituto de Bioquímica Vegetal y Fotosíntesis, cicCartuja, Universidad de Sevialla-CSIC, Avda Americo Vespucio 49, Sevilla 41092, Spain

Supporting Information

ABSTRACT: Post-translational nitration of tyrosine is considered to be an important step in controlling the multiple functions of cytochrome *c* (Cyt-*c*). However, the underlying structural basis and mechanism are not yet understood. In this work, human Cyt-*c* variants in which all but one tyrosine has been substituted by phenylalanine have been studied by resonance Raman and electrochemical methods to probe the consequences of tyrosine nitration on the heme pocket structure and the redox potential. The mutagenic modifications of the protein cause only subtle conformational changes of the protein and small negative shifts of the redox potentials which can be rationalized in terms of long-range electrostatic effects on the heme. The data indicate that the contributions of the individual tyrosines for maintaining the relatively high redox potential of Cyt-*c* are additive. Nitration of individual tyrosines leads to a destabilization of the axial Fe−Met80 bond which causes the substitution of the native Met ligand by a water molecule or a lysine residue for a fraction of the proteins. Electrostatic immobilization of the protein variants on electrodes coated by self-assembled monolayers (SAMs) of mercaptounadecanoic acid destabilizes the heme pocket structure of both the nitrated and non-nitrated variants. Here, the involvement of surface lysines in binding to the SAM surface prevents the replacement of the Met80 ligand by a lysine but instead a His-His coordinated species is formed. The results indicate that structural perturbations of the heme pocket of Cyt-*c* due to tyrosine nitration and to local electric fields are independent of each other and occur via different molecular mechanisms. The present results are consistent with the view that either tyrosine nitration or electrostatic binding to the inner mitochondrial membrane, or both events together, are responsible for the switch from the redox to the peroxidase function.

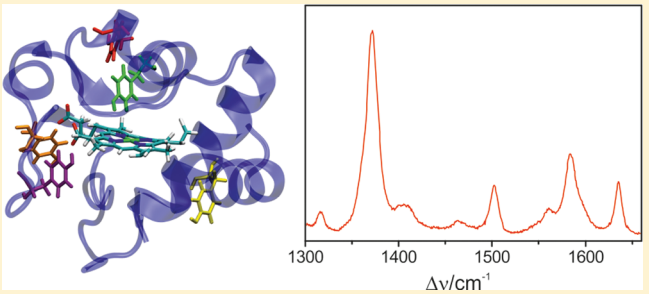

INTRODUCTION

Post-translational modifications of tyrosine residues in proteins represent essential steps for controlling biological functions, frequently related to signaling pathways of cells. Phosphorylation is known to play a key role in a variety of regulatory processes in cell growth, differentiation, and metabolism.[1,2] Nitration of tyrosines has been shown to occur in response to oxidative stress, induced by reaction with NO species.[2−4] The heme protein cytochrome *c* (Cyt-*c*) is one of the target proteins for which both types of tyrosine modifications have been demonstrated and the effects on Cyt-*c*'s biological functions have been widely studied.[5−19]

Cyt-*c* serves as an electron carrier in the mitochondrial intramembrane space transferring electrons from the membrane-bound cytochrome *c* reductase to cytochrome *c* oxidase where molecular oxygen is reduced to water.[20] In addition, Cyt-*c* has been shown to play crucial roles in programmed cell death. In one case, Cyt-*c* binds to the Apaf-1 protein, thereby causing its oligomerization and the subsequent activation of caspases.[21] Prior to this reaction sequence, however, Cyt-*c* has to be transferred through the mitochondrial membrane to the cytosol, a process that is most likely related to the function of Cyt-*c* as a catalyst of H_2O_2-dependent peroxidation of the mitochondria-specific cardiolipin.[22−24]

Nitration of tyrosine residues in Cyt-*c* has been proposed to be the initial event that triggers the change from the biological function in the respiratory chain to apoptosis.[6,14] In fact, in vitro studies revealed an enhanced peroxidase activity for Cyt-*c* upon Tyr nitration,[7,8,13] suggesting a transition from the electron-transfer to cardiolipin-peroxidation function. On the other hand, Tyr nitration inhibits caspase-9 activation and thus blocks the apoptosis signaling pathway.[9,13,15] In this respect, nitration may exert a similar inhibitory effect on caspase as phosphorylation as judged from studies on phosphomimetic Tyr mutants.[18,19]

Received: March 9, 2012
Revised: April 26, 2012
Published: April 27, 2012

Peroxidase activity requires the accessibility of the heme iron by peroxide which is prohibited by the "native" closed heme pocket structure of Cyt-*c* with the axial coordination sites occupied by His18 and Met80. It is thus tempting to relate the catalytically active state of Cyt-*c* to a five-coordinated species lacking the Met80 ligand as it is formed upon electrostatic binding to model membranes.[25−27] Thus, strong electrostatic interactions, possibly in concert with Tyr nitration, have also been suggested to play a key role for the transformation of Cyt-*c* from an electron carrier to a catalyst.[27]

Clearly, a deeper understanding of the functional switch of Cyt-*c* as well as the molecular processes of the protein in apoptosis requires a profound knowledge of the structural consequences of Tyr nitration in Cyt-*c*. Following a previously established approach,[11,13−15] mutants of human Cyt-*c* have been expressed in which four out of five Tyr were substituted by Phe, allowing for a selective nitration of the remaining Tyr (Figure 1). In this work, we have employed resonance Raman

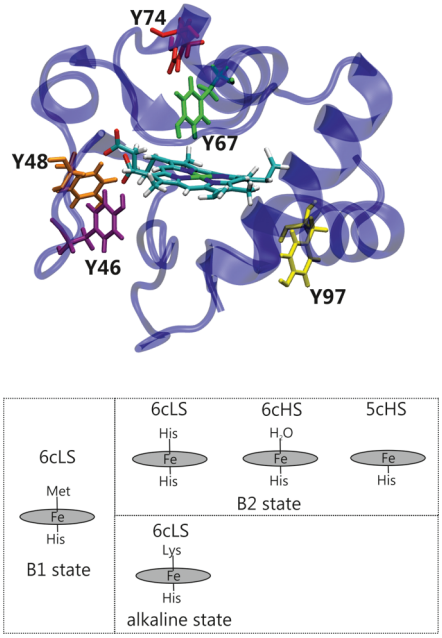

Figure 1. (Top) Three-dimensional structure of human Cyt-*c* (WT)[30] highlighting the heme and the tyrosine residues 46 (violet), 48 (orange), 67 (green), 74 (red), and 97 (yellow). (Bottom) Coordination patterns of the various states of Cyt-*c*.

(RR) spectroscopy to analyze the effect of the mutagenic and chemical modifications on the redox center, specifically the nitration-induced changes in the coordination pattern of the heme. Furthermore, the protein variants were electrostatically immobilized on electrodes coated by self-assembled monolayers (SAMs) of amphiphiles to mimic interactions with negatively charged membranes. Using surface-enhanced resonance Raman (SERR) spectroscopy and cyclic voltammetry (CV), these studies aim at investigating the combined effect of Tyr nitration and electrostatic fields on the heme structure as well as on the redox properties.

MATERIALS AND METHODS

Materials. 11-Mercaptoundecanoic acid (MUA) and sodium peroxodisulfate were purchased from Sigma Aldrich. Potassium hydrogen phosphate, potassium dihydrogen phosphate, potassium hydroxide and sodium dithionite were provided by Fluka (Merck, Germany). Ethanol (99.9%) was obtained from Fischer Scientific Company (Germany). Buffer solutions were prepared using Millipore water (Eschborn, Germany) with a resistance >18 MΩ. All chemicals were used as received.

Expression of Cyt-*c* Mutants. Recombinant human Cyt-*c*, either the *wild-type* species or the monotyrosine mutants in which all tyrosine residues but one (just that at the indicated numbered position, Figure 1) were substituted by phenylalanines, were expressed in *E. coli* DH5α and further purified by ionic exchange chromatography, as previously described.[11,13]

Nitration. Peroxynitrite synthesis and nitration of the different Cyt-*c* samples were carried out as reported previously,[11,13,14] with the following modifications: Fe^{3+}-EDTA concentration and the number of peroxynitrite additions were increased up to 1.5 mM and 10 bolus additions, respectively. The nitration reaction was performed under acidic conditions (pH 5.0). The resulting nitrated Cyt-*c* species were intensively washed with 10 mM potassium phosphate (pH 6.0). Nitrated monotyrosine Cyt-*c* mutants were separated from non-nitrated protein in a CM-cellulose column equilibrated with 1.5 mM borate, pH 9.0, using a 0−100 mM NaCl gradient. Nitrated Cyt-*c* eluted at a much lower salt concentration than native protein because of the extra negative charge of deprotonated tyrosyl anions, whose pK_a is modified by the strong electron-withdrawing effect of the NO_2 substituent at the 3-position.[5] The purity to 95% homogeneity of nitrated Cyt-*c* preparations was corroborated by SDS-Page and Western Blot using antibodies antinitrotyrosine (Biotem) to detect the presence of the NO_2 group. In addition, the molecular mass and the specifically nitrated tyrosine residue of each mutant were confirmed by tryptic digestion and MALDI-TOF (Bruker-Daltonics, Germany) analyses. Samples were concentrated up to 0.2−2.0 mM in 5 mM sodium phosphate buffer (pH 6.0).

Resonance Raman and Surface-Enhanced Resonance Raman Spectroscopy. RR and SERR spectra were acquired using the 413 nm line of a krypton ion laser (Coherent Innova 300c) coupled to a single-stage spectrograph (Jobin Yvon, LabRam 800 HR) equipped with a liquid-nitrogen-cooled back-illuminated CCD detector. The laser beam was focused using a Nikon 20× objective (N.A. 0.35) with a working distance of 20 mm. The laser power on the sample was 1 mW. Acquisition times ranged from 5 to 30 s depending on spectral quality and sample concentration.

RR measurements were carried out in a rotating quartz cuvette. Protein solutions were oxidized and reduced chemically using sodium peroxodisulfate and sodium dithionite, respectively. SERR measurements were conducted in a spectroelectrochemical cell described previously.[28] An electrochemically roughened silver ring (99%, Götz, Germany) coated with a SAM of MUA served as a working electrode. SER activation, SAM coating of the electrode, and subsequent protein immobilization followed the protocol described previously with minor modifications.[28,29] Briefly, prior to experiments the electrolyte solution (50 mM phosphate buffer at pH = 7.0, 9.0, or 12.0) was purged with catalytically purified oxygen-free argon for ca. 20 min. Then, the protein solution was added, yielding a final concentration of ca. 0.2 μM. Protein adsorption was achieved by incubating the working electrode for 30 min into the protein containing buffer solution at open circuit. All SERR experiments were performed in the presence of protein in solution and under Ar overpressure. Potentials cited in this

dx.doi.org/10.1021/jp302301m | J. Phys. Chem. B 2012, 116, 5694−5702

worked refer to an Ag/AgCl (3 M KCl) reference electrode (+0.21 V vs NHE).

Electrochemistry. CV experiments were performed in the spectroelectrochemical SERR cell (vide supra) connected to a CH Instrument 660 C potentiostat (Austin, TX). Determination of peak maxima and baseline subtraction were executed using the CHI software (CHI Electrochemical workstation, Version 6.13).

Molecular Dynamics Simulation. The crystallographic structure of human Cyt-*c* (3NWV)[30] served as template for the molecular dynamics (MD) simulations. The desired mutations and chemical modifications (nitration) were incorporated with VMD 1.8.7.[31] In addition to these sequence changes, each mutant carried a glycine instead of a serine at position 41, which is a naturally occurring apoptosis enhancing mutant.[30] Details of the MD simulations are given in the Supporting Information.

RESULTS

Resonance Raman Spectroscopy. RR spectroscopy is an ideal tool to probe the consequences of protein modifications on the redox center of Cyt-*c*. The present study is restricted to the ferric form of Cyt-*c*, generated by the addition of sodium peroxodisulfate, although in some cases a complete oxidation was not achieved. However, remaining traces of ferrous Cyt-*c* could readily be identified in the experimental spectra on the basis of its strongest band at ca. 1360 cm^{-1}. Besides this minor interference by the ferrous form, the experimental spectra particularly of the Tyr-nitrated protein variants display a substantial heterogeneity as reflected by asymmetric band shapes, shoulders, and extra bands not present in the RR spectrum of the native Cyt-*c* (Figure 2).

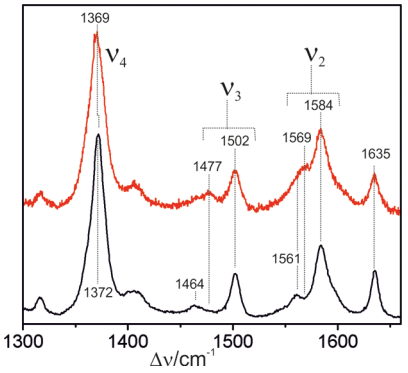

Figure 2. RR spectra of WT Cyt-*c* (bottom) and the Y48-NO_2 variant (top) in the marker band region.

These spectral changes specifically in the region of the modes ν_4, ν_3, and ν_2 indicate contributions from spin and coordination states that differ from the His-Met-coordinated low-spin configuration of the native protein, denoted as state B1.[26] For instance, the broad 1477 and 1569 cm^{-1} bands point to six- and five-coordinated high-spin (6cHS, 5cHS) species and the broadening of the bands at 1502 and 1584 cm^{-1} may originate from non-native six-coordinated low-spin (6cLS) configurations.[26]

In a first attempt to analyze these spectral changes quantitatively, we assumed that mutations and the respective tyrosine nitration solely affect the distribution among different spin and coordination states of the heme whereas the spectra of the individual components are the same in the various protein variants, i.e., the native 6cLS state B1 and the non-native 6cLS, 6cHS, and 5cHS species.[26] However, this component analysis failed to provide a satisfactory global fit to all experimental RR spectra (see Supporting Information). Each of the amino acid substitutions and the respective chemical modification of the single tyrosines cause subtle spectral alterations with frequency changes of ca. ±2 cm^{-1} and intensity variations of ca. 20% for nearly each of the component spectra. Such variations cannot be neglected within a global fit, although they are distinctly smaller than the differences between the component spectra of the individual spin and coordination states.

Thus, we have restricted the RR spectra analysis to the ν_3 band, which is most sensitive to changes of the spin and coordination state of the heme iron, and hence allows for a quantitative analysis in terms of the various coordination states involved. On the basis of a large body of experimental data, the frequency ranges of this band of 1478−1481, 1488−1491, 1500−1502, and 1504−1506 cm^{-1} in the ferric state are indicative of a 6cHS, 5cHS, a Met-His 6cLS, and a "N"-His (N = His, Lys) 6cLS configuration, respectively.[26,32] We thus have employed a band-fitting analysis to this spectral region using four bands with frequencies that were allowed to vary in the above-mentioned ranges in order to take into account the specific effects of the individual mutations and nitration (vide supra) (Figure 3; further details of the band fitting are given in

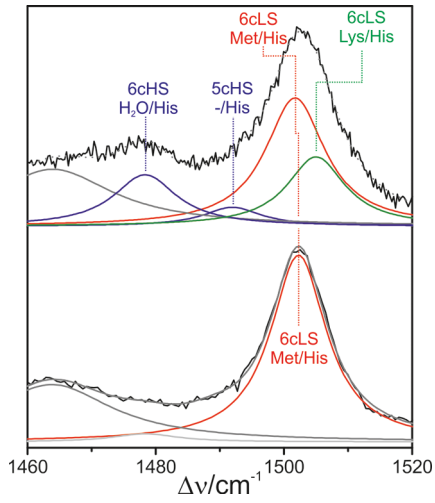

Figure 3. RR spectra in the ν_3 band region of the WT Cyt-*c* (bottom) and the Y46-NO_2 variant (top), including the fitted Lorentzian band shapes.

the Supporting Information). This procedure is associated with a relatively large error for determining weak contributions of the 6cHS state in the presence of a prevailing B1 contribution since the latter species gives rise to a broad band at 1465 cm^{-1} (ν_{28}) that overlaps with the ν_3 mode of the 6cHS state. After taking into account this interference, the relative intensities obtained by the fitting procedure were then converted into relative concentrations (Supporting Information)[33] as listed in Table 1.

The data for the non-nitrated protein variants indicate no changes of the coordination and spin state when all five Tyr (null mutant) are substituted by Phe. This is also true for the monotyrosine variants Y46 and Y74. However, a small but clearly detectable decrease of the native state B1 by ca. 15% is

dx.doi.org/10.1021/jp302301m | J. Phys. Chem. B 2012, 116, 5694−5702

Table 1. Relative Contributions of the Various Spin and Coordination States in Nitrated and Non-nitrated Cyt-*c* Variants (in %)

	native	non-native		
	B1 6cLS (Met-His)	6cLS (Lys-His)	HS[a]	nitration-induced destabilization of the native state B1[b]
WT	100	0	0	–
null	100	0	0	–
Y46	100	0	0	–
Y46-NO_2	42		42	2.4
Y48	85	4	11	–
Y48-NO_2	40	13	47	2.1
Y67	86	0	14	–
Y67-NO_2	57	12	31	1.5
Y74	100	0	0	–
Y74-NO_2	63	13	24	1.6
Y97	92	1	7	–
Y97-NO_2	90	4	6	1.0

[a]The contribution of the 5cHS (-His) and 6cHS (H_2O-His) were combined. [b]Ratio of the contributions of the native state in the non-nitrated and nitrated forms

noted for Y67 and Y48 and by 8% for Y97. The situation is different when the single Tyr residues are nitrated. These modifications lead to a significant population of a non-native 6cLS and a HS configuration (predominantly 6cHS) with a relative contribution of ca. 15% and between 25 and 45%, respectively. The only exception refers to Y97-NO_2, in which the nitration site (i.e., the tyrosine) is most remote from the heme (Supporting Information). Here the relative contributions of the non-native species are distinctly lower and are, within the fitting accuracy, unchanged compared to the non-nitrated protein.

The non-native 6cLS state is of particular interest since the nature of the "new" axial ligand that has replaced Met80 is not clear a priori. The position of the marker bands ν_3 (vide supra) or ν_{10} indicate the coordination via a nitrogen atom that may either be provided by a His or by a Lys. In the former case, His33 or His26 may be potential candidates since these amino acids have been identified as axial ligands in an (metastable) intermediate formed during unfolding or refolding.[34] This coordination pattern is also found in Cyt-*c* electrostatically bound to negatively charged surfaces, denoted as state B2 in distinction to state B1 as the native state.[26] Alternatively, a Lys (72, 73, or 79) may bind to the heme iron corresponding to the "alkaline" state typically formed for WT Cyt-*c* at a pH above 10.[35,36]

We have, therefore, examined the low-frequency region of the RR spectra to distinguish between both possibilities. In this region, the alkaline state and state B2 each exhibits a unique band pattern that differs from the characteristic RR spectrum of the native Met-His coordinated 6cLS state (B1) and are not superimposed by the intrinsically weak RR bands of the HS species.[35,37] Nevertheless, the relatively low relative contributions of the non-native 6cLS form require a difference procedure to enhance the spectral changes with respect to the native state.

First, the WT protein was measured at pH 7 and pH 12 to obtain the native B1 state and a largely pure alkaline state. The

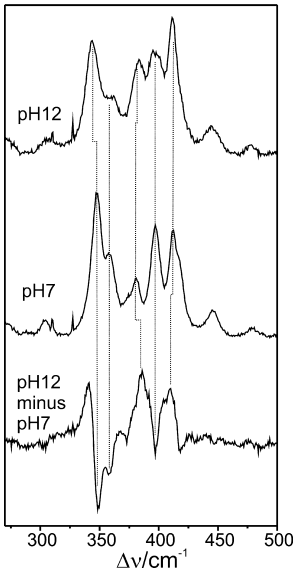

Figure 4. Low-frequency RR spectra of WT Cyt-*c* at pH 12 and at pH 7. The third trace displays the difference spectrum "pH 12 minus pH 7".

difference spectrum "pH12 minus pH7" in this region displays a characteristic pattern of positive and negative signals (Figure 4), which is also found for the null mutant and all non-nitrated Cyt-*c* variants, indicating that in each mutant the alkaline form with its characteristic Lys/His axial coordination pattern of the heme prevails at pH 12. To find out whether the non-native 6cLS state, which is partially populated upon Tyr nitration in neutral solutions, exhibits the same Lys/His coordination as the alkaline form, we have constructed the difference spectra "nitrated monotyrosine mutant minus non-nitrated monotyrosine mutant" from the spectra measured at pH 7. In fact, the difference spectra for all tyrosine mutants (i.e., "nitrated" minus "non-nitrated") display band patterns, which are similar to that of the "pH12 minus pH7" difference spectrum of WT Cyt-*c* or the "null" mutant (Figure 5). These findings suggest that in the nitrated variants the N-containing ligand of the "N"/His 6cLS species is a Lys.

UV−Vis Absorption Spectroscopy. The effect of the Tyr-to-Phe substitutions on the absorption spectra of the non-nitrated Cyt-*c* variants in the Soret band region is relatively small (ca. <3 nm), whereas upon nitration the peak maximum is shifted more significantly to the blue by up to 6 nm (Supporting Information). These shifts mainly reflect the coexistence of different spin and coordination states and specifically the formation of a HS species which is known to exhibit a Soret band maximum at wavelengths shorter than the 6cLS forms. Thus, the UV−vis absorption data are in agreement with the RR spectroscopic results inasmuch as the largest blue shift of the Soret maximum is noted for Y46-NO_2 and Y48-NO_2 which includes the largest HS contribution, in agreement with previous reports.[14,15]

Surface-Enhanced Resonance Raman Spectroscopy. To probe electric field effects on the protein stability, Cyt-*c* variants were electrostatically immobilized on an Ag electrode coated with a carboxyl-terminated SAM of MUA and studied by SERR spectroscopy. The SERR spectrum of WT Cyt-*c* is

dx.doi.org/10.1021/jp302301m | J. Phys. Chem. B 2012, 116, 5694−5702

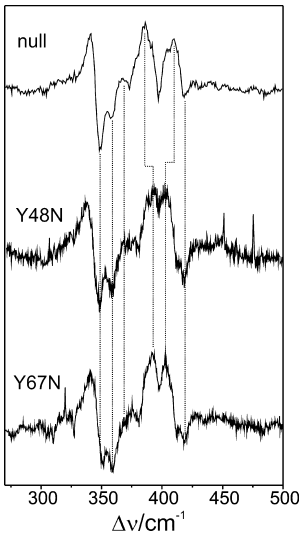

Figure 5. Difference spectrum "pH 12 minus pH 7" of the null mutant compared with the difference spectra of Y48-NO_2 and Y67-NO_2 obtained from the spectra of the respective nitrated mutants and the non-nitrated mutant, all measured at pH 7.

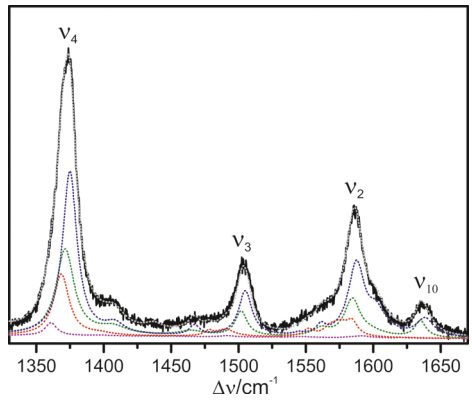

Figure 6. SERR spectrum of the null variant of Cyt-*c* obtained from a MUA-coated Ag electrode, including the component spectra obtained by a global fit. The component spectra of the oxidized B1, reduced B1, the oxidized B2[6cLS], and the oxidized B2[HS] (sum of the 5cHS and 6cHS species) are given by the dotted lines in green, magenta, blue, and red, respectively. The dotted gray line represents the sum of the component spectra.

Table 2. Relative Contributions (in %) of the Various Spin and Coordination States of Cyt-*c* Variants Immobilized on SAM-Coated Electrodes at +0.15 V

	B1 6cLS (Met-His)	B2 6cLS (His-His)	B2HS[a]	electric-field-induced destabilization of the native state B1[b]
WT	76	16	8	1.3
null	49	39	12	2.0
Y46	42	17	41	2.3
Y46-NO_2	30	24	46	1.4
Y48	42	42	16	2.0
Y48-NO_2	43	43	14	0.9
Y67	51	41	8	1.7
Y67-NO_2	42	43	15	1.4
Y74	64	20	16	1.6
Y74-NO_2	45	42	13	1.4
Y97	42	26	32	2.2
Y97-NO_2	33	21	46	2.7

[a]The contributions of the 5cHS (-His) and 6cHS (H_2O-His) were combined. [b]Ratio of the contributions of the native state in solution (Table 1) and in the immobilized state.

dominated by the component spectrum of the native state B1 which is nearly identical to the RR spectrum of the protein in solution. This state could be reversibly oxidized and reduced by varying the electrode potential. Thus, the behavior of the human WT Cyt-*c* on MUA-coated electrodes is similar to that of horse heart protein except for a higher contribution of non-native states in the SERR spectrum of human Cyt-*c*.[28]

Unlike the RR spectroscopic analysis of the proteins in solution, a global component analysis could be applied starting with the component spectra previously determined for horse heart Cyt-*c*.[26,28] Only minor adjustments of a few spectral parameters (i.e., intensities in the ν_2 region) were required to improve the global fit. Thus, all experimental spectra could be simulated by the same set of component spectra, i.e., the spectra of the native reduced and oxidized B1 state (6cLS with Met-His ligation) and the oxidized B2 species including the 5cHS (−/His) and 6cHS (H_2O/His) configuration as well as the 6cLS ("N"/His) configuration (see Supporting Information). The component spectrum of the latter is nearly identical to that of the bis(histidine)-coordinated 6cLS state of horse heart Cyt-*c* implying that, unlike the proteins in solution, an additional His (instead of a Lys) serves as the sixth ligand in the immobilized nitrated and non-nitrated Tyr variants. Spectra of the reduced forms of the B2 species were not required for the global fit since the experiments were carried out above the respective reduction potentials between −0.25 and −0.4 V (vs AgCl).[38] Figure 6 shows an example of a SERR spectrum analyzed in this way. The resultant relative weights of the individual component spectra were then converted into relative concentrations (Table 2) according to the procedure described previously (Supporting Information)[33] such that the data can be directly compared with those obtained for Cyt-*c* in solution on the basis of the ν_3 band fitting (Table 1). However, the accuracy of the component analysis is significantly higher than for a simple band fitting analysis since complete spectra of the individual components are fitted to the experimental spectra and the degrees of freedom in the fitting procedure are restricted to the number of components.[39] Further data on the distribution among the various states at open circuit of the electrode are given in the Supporting Information.

Electrochemistry. The formal midpoint potential and the electron-transfer rate constants of the various Cyt-*c* variants immobilized on SAM-coated Ag electrodes were measured by CV using a potential range from +0.15 to −0.2 V. Under these conditions, CV solely probes the redox potentials of the native B1 state since, according to the previous findings for horse heart Cyt-*c*, the B2 species should give rise to redox potentials lower than −0.2 V.[38] Extending this conclusion from horse heart to human Cyt-*c* is justified in view of the far-reaching similarities in the three-dimensional structures[30,40] and the spectral properties, including the RR spectra (vide supra). Also, the midpoint potentials of the immobilized WT proteins have been found to be essentially the same with 22 and 23 mV for horse heart and human Cyt-*c*, respectively.[28,41]

dx.doi.org/10.1021/jp302301m | J. Phys. Chem. B 2012, 116, 5694−5702

The CVs afforded well-resolved peaks and a quasi-reversible electron transfer (ET), reflected by a full width at half-height of

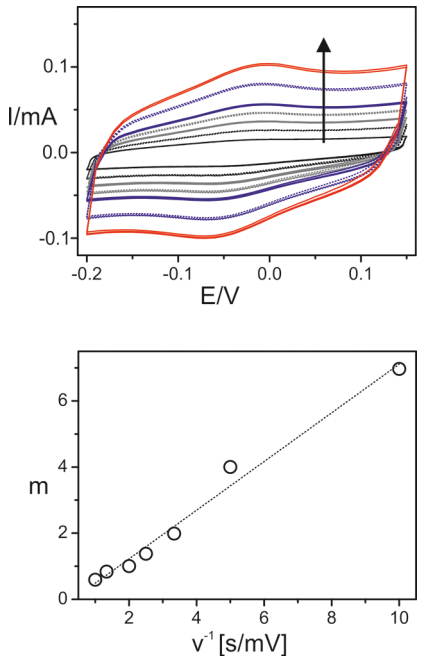

Figure 7. CVs of WT human Cyt-*c* (top) obtained with increasing scan rates (in the direction of the arrow, 100, 200, 300, 400, 500, 750, and 1000 mV/s) and the Laviron plot (bottom).

Table 3. Redox Properties of the Non-nitrated and Nitrated Cyt-*c* Variants Immobilized on a MUA-Coated Ag Electrode

protein	E^0/mV	k_{ET}/s^{-1}
WT	22	4
null	−33	29
Y46	−24	59
Y46-NO_2	−46	31
Y48	−13	10
Y48-NO_2	−61	28
Y67	−2	7
Y67-NO_2	−5	27
Y74	−28	60
Y74-NO_2	−20	40
Y97	−22	32
Y97-NO_2	−31	53

80−100 mV (Figure 7). Upon mutation the redox potential is significantly lowered by up to 50 mV (Table 3). Additional downshifts of the redox potential were noted upon tyrosine nitration except for the Y74 protein which displays a small upshift in the Y74-NO_2 variant.

Upon varying the scan rate, the ET kinetics of the immobilized Cyt-*c* variants has been determined by applying the Laviron method (Figure 7). The ET rate constant of the WT protein was found to be distinctly smaller compared to that determined for horse heart Cyt-*c* under otherwise the same conditions (4 vs 40 s^{-1}).[41] The mutation of the individual tyrosines leads to a strong increase of the ET rate constant whereas nitration either accelerates or slows down the heterogeneous ET.

DISCUSSION

Effect of Phe-to-Tyr Mutations on the Redox Center.

The most striking result of the RR spectroscopic analysis of the non-nitrated Cyt-*c* is the fact that substitutions of all Tyr by Phe leaves the redox site structure essentially unchanged whereas preservation of a single Tyr residue in position 48, 67, or 97 causes a weakening of the Fe−Met bond and thus leads to small contributions of non-native states. These results are difficult to rationalize since one intuitively expects that specifically Tyr67, due to its proximity to the heme, exerts a stabilizing function on the heme pocket. We thus conclude that the small effects on the coordination state of Cyt-*c* (as well as on the small spectral modifications of the respective native B1 state) are largely due to long-range perturbations of the electrostatics in the heme pocket. In some cases, such as the null mutant, the structural consequences of individual Tyr-to-Phe substitutions may accidentally compensate each other. However, it should be noted that this conclusion solely refers to the structure of the heme site as the RR spectra do not provide information about structural changes of protein.

The situation is different for the effect of the individual tyrosine residues on the redox potential of the heme in the native state B1. All the monotyrosine mutants, including the null variant, display negative shifts of the redox potential with respect to the WT protein (Table 3). Assuming that each Tyr residue exerts an incremental contribution to the redox potential, one may express the redox potential shift ΔE_i for each variant i according to

$$\Delta E_i = E_i^0 - E_{WT}^0 = \sum_j \varepsilon_{i,j} \quad (1)$$

where E_{WT}^0 and E_i^0 are the redox potentials of the WT protein and mono-Tyr variant i, respectively, and $\varepsilon_{i,j}$ represents the incremental redox potential shift due to the Tyr-to-Phe substitution at the amino acid position j; i.e., $\varepsilon_{i,j}$ is zero for $i = j$ but nonzero for $i \neq j$. Correspondingly, one obtains a set of five equations according to the scheme in Table 4 that can be solved to afford the individual values for ε_j. This approach is justified a posteriori since the sum of all ε_j values is very similar

Table 4. Shifts of the Redox Potential of Non-nitrated Protein Variants and Contributions of the Individual Tyr Residues[a]

	tyrosine residues					
protein	67	48	46	74	97	ΔE^0/mV
WT	x	x	x	x	x	0
Y67	x	–	–	–	–	−24
Y48	–	x	–	–	–	−35
Y46	–	–	x	–	–	−46
Y74	–	–	–	x	–	−50
Y97	–	–	–	–	x	−44
null	–	–	–	–	–	−55
	ε_{67}	ε_{48}	ε_{46}	ε_{74}	ε_{97}	$\sum_j \varepsilon_j$
contribn to ΔE^0 (in mV)	−25.75	−14.75	−3.75	0.25	−5.75	−49.75
contribn to ΔE^0 (in mV) for the nitrated Tyr	−41.25	+14.75	−0.25	−26.25	−15.25	−68.25
distance to the heme (Å)	6.5	10.2	9.4	12.6	14.0	

[a]Determined according to eq 1.

dx.doi.org/10.1021/jp302301m | J. Phys. Chem. B 2012, 116, 5694−5702

(−50 mV) to the redox potential shift of the null mutant of −55 mV. This finding suggests that the main origin of the redox potential shifts lies in a change of the polarity and electrostatics of the protein environment rather than a mutation-induced structural perturbation of the redox center. This conclusion is consistent with the appreciable long-range effect of the most remote Tyr residue at position 97, although those residues that are in closest proximity to the heme (i.e., at positions 67 and 48) exert the strongest influence on the redox potential.

The redox potentials determined in this work refer to the native B1 state of the proteins immobilized on the MUA-coated Ag electrode. Taking into account the interfacial potential drop which leads to a small apparent negative shift of the redox potentials,[28] the values for the WT protein and the null variant are in good agreement with those in solution.[11] However, redox potential shifts of the mono-Tyr mutants differ slightly for the protein in solution and on the electrode (Supporting Information) which may be attributed to the distance- and orientation-dependent modulation of ε_j by the interfacial electric field.[42]

Effect of Tyrosine Nitration on the Redox Center. Upon nitration, a considerable fraction of the individual Tyr variants is converted into states with non-native heme coordination. Among them, a new 6cLS species is formed with ca. 15% in all nitrated Cyt-*c* variants except for Y97-NO_2 (<10%). RR spectra indicate that this 6cLS species is closely related the alkaline form of Cyt-*c* in which Met80 is replaced by a Lys (72, 73, or 79). These findings are in agreement with previous spectroscopic data on the nitrated Tyr mutants.[12−14] In WT Cyt-*c*, this alkaline species is formed at a pH above 9.5,[13] corresponding to the pK_a of the surface-exposed lysine residues. Thus, deprotonation of the Lys side chain is likely to be the crucial step of this conformational transition and the stronger binding affinity of the Lys amino group to the ferric heme compared to the thioether group of Met80 may constitute a significant thermodynamic driving force. However, formation of the Lys/His coordinated species in the nitrated Tyr mutants of Cyt-*c* at pH 7 seems to follow a different mechanism in view of the concomitant formation of the prevailing 6cHS species which is attributed to a H_2O/His heme (Table 1). The coexistence of the 6cLS and the HS form detected in the present RR spectroscopic study suggests that the primary effect of tyrosine nitration is the destabilization of the native state B1, specifically the weakening of Fe−S(Met80) bond, rather than a lowering of the pK_a of one of the surface lysines.

Nitration of the tyrosines does not display a uniform tendency for the individual redox potential shifts of the B1 state of immobilized protein (Table 3) which can be analyzed according to eq 1. Whereas ε_j for the nitrated Tyr at positions 67, 74, and 97 is distinctly more negative than for the non-nitrated form, the value for ε_{46} remains small. Most strikingly, however, there is a large positive shift for ε_{48} by 30 mV compared to the non-nitrated Tyr. Note that in solution most of the nitrated mono-Tyr mutants display a positive redox potential shift compared to the non-nitrated forms.[11]

Coordination State Changes and Peroxidase Activity. Previous studies have shown that Tyr nitration leads to an increase of the peroxidase activity.[7,13] Intuitively, one might expect a direct correlation between the peroxidase activity and the relative contribution of the HS species with its vacant (or only weakly bound) axial coordination site, which increases in the order Y48-NO_2 ≈ Y46-NO_2 > Y74-NO_2 ≈ Y67-NO_2 > Y97-NO_2 (Table 1). The same order holds for the nitration-induced destabilization of the native B1 state in general. For Y46-NO_2, Y48-NO_2 and Y74-NO_2 but not for Y67-NO_2 a significantly increased peroxidase activity was found.[13,14] Also, the comparison with the enzymatic data for the site-specifically nitrated wild-type Cyt-*c* reported by Batthány et al.[7] does not provide an unambiguous correlation with the present spectroscopic results on the corresponding monotyrosine mutants inasmuch as the peroxidase activity follows the order Y74-NO_2 > Y67-NO_2 ≈ Y97-NO_2. Accordingly, it appears to be more plausible to assume that the peroxidase process is primarily controlled by the accessibility of the heme pocket for H_2O_2 which requires a destabilization of the heme crevice.[13] This conclusion is in line with a previous UV RR study by Spiro and co-workers.[43] These structural changes are accompanied by a weakening of the Fe-Met bond which eventually may lead to the removal of the ligand from the heme.[14]

Effect of the Electric Field on the Redox Site. The relationship between destabilization of the heme crevice and the distortion of the axial heme coordination has been observed for Cyt-*c* bound to negatively charged liposomes including cardiolipin or other anionic phospholipids,[23,25,26,44,45] or even more simple membranes models such as an electrode coated by a SAM with anionic head groups.[26−28,41] Thus, it has been assumed that also electrostatic interactions, which govern Cyt-*c* binding to the cardiolipin-rich inner mitochondrial membrane, may promote the switch from the redox to the peroxidase function.[41] In these electrostatic complexes, however, the weakening of the Fe-Met leads to a 5cHS and a new non-native 6cLS state in which a His (33 or 26) replaces the Met80 ligand of the heme iron (B2 states).[26−28] In fact, also the non-nitrated and nitrated protein variants of human Cyt-*c* immobilized on SAM-coated electrodes show a similar behavior. The component spectrum of the 6cLS species in the present SERR spectra is essentially identical to that of the B2 6cLS state of horse heart Cyt-*c*.[26] Conversely, the alternative assignment of this species to the alkaline state is rather unlikely since the Lys residues that might substitute the Met80 ligand are involved in electrostatic binding of the protein to the SAM surface.[46]

The extent of B2 formation, including both the 6cLS and the HS forms, is higher for the human WT Cyt-*c* protein than for the WT Cyt-*c* from horse heart under similar experimental conditions but it is further increased for the various Tyr mutants, including the null mutant. For the non-nitrated variants, the interfacial electric field induces a decrease of the B1 content by a factor of ca. 2. This factor is distinctly higher than for the WT protein and the average value for the nitrated Tyr mutants (1.3), except for Y97-NO_2, such that the contribution of the native B1 state has dropped to a similar value of ca. 40% in all nitrated and non-nitrated mutants. These findings suggest that the electric-field-induced destabilization of the redox site is largely independent of the site of the Tyr → Phe substitutions and the Tyr nitration. In fact, the strength of the electrostatic interactions and thus the electric field experienced by the bound proteins seem to remain largely unchanged since the various Tyr → Phe substitutions and the respective nitrations do not affect the charge distribution in the binding domain and do not significantly alter the dipole moment of the protein (Supporting Information).

The dipole moment of ferric human WT Cyt-*c* has been calculated to be 254 D in the present work (Supporting Information) and thus is distinctly higher than that of horse WT horse heart Cyt-*c* (184 D),[47] implying that electrostatic

interactions on the MUA-coated Ag electrode are much stronger for the human protein. One consequence refers to the electric-field-induced stabilization of the heme pocket which is more severe for human WT Cyt-*c* (24% B2; Table 2) than for horse heart Cyt-*c* (~0% B2)[28] under the same immobilization conditions. Consistently, destabilization of yeast iso-1 Cyt-*c*, which exhibits a dipole moment 544 D in the ferric form,[47] is even more severe than for human Cyt-*c*. The second consequence is related to the electron-transfer process in the immobilized state which has been shown to be controlled by the interplay between protein dynamics and electron tunneling.[27,41,46,48] Since the thermodynamically preferred binding domain of Cyt-*c* does not correspond to the orientation that is optimum for electron transfer, a reorientation of the bound protein must precede electron tunneling which is the rate-limiting step for horse heart Cyt-*c* on a MUA-coated Ag electrode (k_{ET} = 40 s^{-1}). With increasing strength of electrostatic binding, reorientation is slowed down and may become the rate-limiting step as it is most likely the case for WT human Cyt-*c* (k_{ET} = 4 s^{-1}; Table 3). For yeast iso-1 Cyt-*c*, the strong electrostatic binding to the MUA surface even impairs the spectroelectrochemical determination of the interfacial electron transfer.[47] On the other hand, the increase of the electron-transfer rate constant upon Tyr → Phe substitution and Tyr nitration cannot be related to the relatively small changes of the dipole moment by less than 10% compared to the WT protein (Supporting Information). More detailed experimental and theoretical studies are required to explore the impact of the mutational and chemical modifications of Cyt-*c* on the dynamics and the electron tunneling pathways in the immobilized state.

CONCLUSIONS

The effect of Tyr nitration on the structural and redox properties of the heme site of Cyt-*c* was studied on the basis of mono-Tyr mutants. This approach is based on the approximation that the replacement of Tyr by Phe only causes minor perturbations of the protein structure and the redox potential. This assumption seems to be largely justified since crucial structural parameters of the heme pocket are preserved, including the sensitive Fe−Met axial bond. The RR spectroscopic analysis reveals subtle conformational changes beyond the level of heme ligand exchange, which are, however, accompanied by redox potential shifts by up to −55 mV. Most surprisingly, the effects of the individual Tyr → Phe substitutions on the redox potential are additive, pointing to long-range electrostatic perturbations of the redox potential.

Nitration of the individual tyrosines causes more severe structural changes of the heme pocket including a substantial weakening of the Fe-Met axial bond which eventually leads to partial formation of non-native ligation states. These states include HS species and a Lys-His coordinated 6cLS species at pH 7.0 with the same coordination pattern as the alkaline form of the WT and the non-nitrated Cyt-*c* variants formed above pH 10.0. There is no direct correlation between the peroxidase activity determined previously[7,13] and the relative contribution of the HS forms or with the extent of coordination state changes in toto. These findings support the view that nitration-induced peroxidase activity is primarily due to the increased accessibility of H_2O_2 which results from the perturbation of the heme crevice.

Upon electrostatic binding to SAM-coated electrodes, the Fe−Met axial bond is weakened for both the nitrated and non-nitrated protein variants to a comparable extent implying that the electric-field-induced destabilization of the heme pocket structure is largely independent of the effect of tyrosine nitration. In the immobilized state, a Lys-His coordinated species is not formed due to the involvement of Lys residues in electrostatic binding to the SAM surface, but instead His33 (or His26) evidently replaces Met80 to form a non-native 6cLS state. The same structural changes, albeit not so pronounced, are also observed for the WT protein.

Both Tyr nitration and membrane binding cause similar albeit not identical destabilizations of the heme pocket, leading to a decrease of the native B1 conformation. In both cases, the non-native states, i.e., the HS forms, the alkaline-like species in solution, and the His-His coordinated 6cLS form in the immobilized state, display a strongly negatively shifted redox potential[25,28,38,49] that impairs electron acceptance from cytochrome *c* reductase. Thus, the present results are consistent with the view that either Tyr nitration or electrostatic binding to the anionic cardiolipin-rich inner mitochondrial membrane, or the combination of both events, may trigger the functional switch from the redox to the peroxidase function of Cyt-*c*.

ASSOCIATED CONTENT

Supporting Information

The material includes a description of the RR and SERR spectroscopic analysis, UV−vis absorption spectra, and details of the MD simulations. This material is available free of charge via the Internet at http://pubs.acs.org.

AUTHOR INFORMATION

Corresponding Author

*E-mail: hildebrandt@chem.tu-berlin.de. Tel.: +49-30-314-21419.

Notes

The authors declare no competing financial interest.

ACKNOWLEDGMENTS

The authors thank the Spanish Ministry of Science and Innovation (BFU2009-07190) and the Andalusian Government (BIO198) for financial support. The work was further supported by the Cluster of Excellence "Unifying Concepts in Catalysis" funded by the DFG.

ABBREVIATIONS

CV, cyclic voltammetry; Cyt-*c*, cytochrome *c*; HS, high spin; LS, low spin; MD, molecular dynamics; MUA, mercaptoundecanoic acid; RR, resonance Raman; SAM, self-assembled monolayer; SERR, surface enhanced resonance Raman

REFERENCES

(1) Tarrant, M. K.; Cole, P. A. *Annu. Rev. Biochem.* **2009**, *78*, 797−825.
(2) Monteiro, H. P.; Arai, R. J.; Travassos, L. R. *Antiox. Red. Sign.* **2008**, *10*, 843−889.
(3) Ischiropoulos, H. *Biochem. Biophys. Res. Commun.* **2003**, *305*, 776−783.
(4) Koeck, T.; Fu, X.; Hazen, J. W.; Crabb, J. W.; Stuehr, D. J.; Aulak, K. S. *J. Biol. Chem.* **2004**, *279*, 27257−27262.
(5) Cassina, A. M.; Hodara, R.; Souza, J. M.; Thomson, L.; Castro, L.; Ischiropoulos, H.; Freeman, B. A.; Radi, R. *J. Biol. Chem.* **2000**, *275*, 21409−21415.
(6) Radi, R. *Proc. Natl. Acad. Sci. U.S.A.* **2004**, *101*, 4003−4008.

(7) Batthyány, C.; Souza, J. M.; Durán, R.; Cassina, A.; Cerveñansky, C.; Radi, R. *Biochemistry* **2005**, *44*, 8038−8046.
(8) Jang, B.; Han, S. *Biochimie* **2005**, *88*, 53−58.
(9) Nakagawa, H.; Komai, N.; Takusagawa, M.; Miura, Y.; Toda, T.; Miyata, N.; Ozawa, T.; Ikota, N. *Biol. Biol. Pharm. Bull.* **2007**, *30*, 15−20.
(10) Souza, J. M.; Castro, L.; Cassina, A. M.; Batthyány, C.; Radi, R. *Methods Enzymol.* **2008**, *441*, 197−215.
(11) Rodríguez-Roldán, V.; García-Heredia, J. M.; Navarro, J. A.; De la Rosa, M. A.; Hervás, M. *Biochemistry* **2008**, *47*, 12371−12379.
(12) Abriata, L. A.; Cassina, A.; Tórtora, V.; Marín, M.; Souza, J. M.; Castro, L.; Vila, A. J.; Radi, R. *J. Biol. Chem.* **2009**, *284*, 17−26.
(13) García-Heredia, J. M.; Díaz-Moreno, I.; Nieto, P. M.; Orzáez, M.; Kocanis, S.; Teixeira, M.; Pérez-Payá, E.; Díaz-Quintana, A.; De la Rosa, M. A. *Biochim. Biophys. Acta* **2010**, *1797*, 981−983.
(14) Díaz-Moreno, I.; García-Heredia, J. M.; Díaz-Quintana, A.; Teixeira, M.; De la Rosa, M. A. *Biochim. Biophys. Acta* **2011**, *1807*, 1616−1623.
(15) García-Heredia, J. M.; Díaz-Moreno, I.; Díaz-Quintana, A.; Orzáez, M.; Navarro, J. A.; Hervás, M.; De la Rosa, M. A. *FEBS Lett.* **2012**, *586*, 154−158.
(16) Lee, I.; Salomon, A. R.; Yu, K.; Doan, J. W.; Grossman, L. I.; Hüttemann, M. *Biochemistry* **2006**, *45*, 9121−9128.
(17) Yu, H.; Lee, I.; Salomon, A. R.; Yu, K.; Hüttemann, M. *Biochim. Biophys. Acta* **2008**, *1777*, 1066−1071.
(18) Pecina, P.; Borisenko, G. G.; Belokova, N. A.; Tyurina, Y. Y.; Pecinova, A.; Lee, I.; Samhan-Arias, A. K.; Przyklenk, K.; Kagan, V. E.; Hüttemann, M. *Biochemistry* **2010**, *49*, 6705−6714.
(19) García-Heredia, J. M.; Díaz-Quintana, A.; Salzano, M.; Orzáez, M.; Pérez-Payá, E.; Teixeira, M.; De la Rosa, M. A.; Díaz-Quintana, A. *J. Biol. Inorg. Chem.* **2011**, *16*, 1155−1168.
(20) Scott, R. A., Mauk, A. G., Eds. *Cytochrome c—a multidisciplinary approach*; University Science Books: Sausalito, CA, 1995.
(21) Ow, Y. L.; Green, D. R.; Hao, Z.; Mak, T. W. *Nat. Rev. Mol. Cell Biol.* **2008**, *9*, 532−542.
(22) Kagan, V. E.; Tyurin, V. A.; Jiang, J.; Tyurina, Y. Y.; Ritov, V. B.; Amoscato, A. A.; Osipov, A. N.; Belikova, N. A.; Kapralov, A. A.; Kini, V.; et al. *Nat. Chem. Biol.* **2005**, *4*, 223−232.
(23) Belikova, N. A.; Vladimorov, Y. A.; Osipov, A. N.; Kapralov, A. A.; Tyurin, V. A.; Potapovich, M. V.; Basova, L. V.; Peterson, J.; Kurnikov, I. V.; Kagan, V. E. *Biochemistry* **2006**, *45*, 4998−5009.
(24) Kagan, V. E.; Bayir, A.; Bayir, H.; Stoyanovsky, D.; Borisenko, G. G.; Tyurina, Y. Y.; Wipf, P.; Atkinson, J.; Greenberger, J. S.; Chapkin, R. S.; et al. *Mol. Nutr. Food Res.* **2009**, *53*, 104−114.
(25) Basova, V. L.; Kurnikov, I. V.; Wang, L.; Ritov, V. B.; Belikova, N. A.; Vlasova, I. I.; Pacheco, A. A.; Winnica, D. E.; Peterson, J.; Bayir, H.; et al. *Biochemistry* **2007**, *46*, 3423−3434.
(26) Oellerich, S.; Wackerbarth, H.; Hildebrandt, P. *J. Phys. Chem. B* **2002**, *106*, 6566−6580.
(27) Ly, H. K.; Sezer, M.; Wisitruangsakul, N.; Feng, J. J.; Kranich, A.; Millo, D.; Weidinger, I. M.; Zebger, I.; Murgida, D. H.; Hildebrandt, P. *FEBS J.* **2011**, *278*, 1382−1390.
(28) Murgida, D. H.; Hildebrandt, P. *J. Phys. Chem. B* **2001**, *105*, 1578−1586.
(29) Wackerbarth, H.; Klar, U.; Günther, W.; Hildebrandt, P. *Appl. Spectrosc.* **1999**, *53*, 283−291.
(30) Liptak, M. D.; Fagerlund, R. D.; Ledgerwood, E. C.; Wilbanks, S. M.; Bren, K. L. *J. Am. Chem. Soc.* **2011**, *133*, 1153−1155.
(31) Humphrey, W.; Dalke, A.; Schulten, K. *J. Mol. Graph.* **1996**, *14*, 33−38.
(32) Parthasarathi, N.; Hansen, C.; Yamaguchi, S.; Spiro, T. G. *J. Am. Chem. Soc.* **1987**, *109*, 3865−3871.
(33) Oellerich, S.; Wackerbarth, H.; Hildebrandt, P. *Eur. Biophys. J.* **2003**, *32*, 599−613.
(34) Yeh, S. R.; Han, S. W.; Rousseau, D. L. *Acc. Chem. Res.* **1998**, *31*, 7276−7280.
(35) Döpner, S.; Hildebrandt, P.; Rosell, F. I.; Mauk, A. G. *J. Am. Chem. Soc.* **1998**, *120*, 11246−11255.
(36) Pollock, W. B. R.; Rosell, F. I.; Twitchett, M. B.; Dumont, M. E.; Mauk, A. G. *Biochemistry* **1998**, *37*, 6124−6131.
(37) Hildebrandt, P. *Biochim. Biophys. Acta* **1990**, *1040*, 175−186.
(38) Wackerbarth, H.; Oellerich, S.; Hildebrandt, P. *Chem. Phys. Chem.* **2003**, *4*, 714−724.
(39) Döpner, S.; Hildebrandt, P.; Mauk, A. G.; Lenk, H.; Stempfle, W. *Spectrochim. Acta Part A, Biomol. Spectrosc.* **1996**, *51*, 573.
(40) Bushnell, G. W.; Louie, G. V.; Brayer, G. D. *J. Mol. Biol.* **1990**, *214*, 585−595.
(41) Ly, K. H.; Wisitruangsakul, N.; Sezer, M.; Feng, J. J.; Kranich, A.; Weidinger, I.; Zebger, I.; Murgida, D. H.; Hildebrandt, P. *J. Electroanal. Chem.* **2011**, *660*, 367−376.
(42) Rivas, L.; Soares, C. M.; Baptista, A. M.; Simaan, J.; DiPaolo, R.; Murgida, D. H.; Hildebrandt, P. *Biophys. J.* **2005**, *88*, 4188−4199.
(43) Balakrishnan, G.; Hu, Y.; Oyerinde, O. F.; Su, J.; Grooves, J. T.; Spiro, T. G. *J. Am. Chem. Soc.* **2006**, *129*, 504−505.
(44) Oellerich, S.; Lecomte, S.; Paternostre, M.; Heimburg, T.; Hildebrandt, P. *J. Phys. Chem. B* **2004**, *108*, 3871−3878.
(45) Kapralov, A. A.; Kurnikov, I. V.; Vlasova, I. I.; Belikova, N. A.; Tyurin, V. A.; Basova, L. V.; Zhao, Q.; Tyurina, Y. Y.; Jiang, J.; Bayir, H.; et al. *Biochemistry* **2007**, *46*, 14232−14244.
(46) Paggi, D. A.; Martín, D. F.; Kranich, A.; Hildebrandt, P.; Martí, M.; Murgida, D. H. *Electrochim. Acta* **2009**, *54*, 4963−4970.
(47) Feng, J. J.; Murgida, D. H.; Utesch, T.; Mroginski, M. A.; Hildebrandt, P.; Weidinger, I. *J. Phys. Chem. B.* **2008**, *112*, 15202−15211.
(48) Kranich, A.; Ly, H. K.; Hildebrandt, P.; Murgida, D. H. *J. Am. Chem. Soc.* **2008**, *130*, 9844−9848.
(49) Barker, P. D.; Mauk, A. G. *J. Am. Chem. Soc.* **1992**, *114*, 3619−3624.